MJFAS Malaysian Journal of Fundamental and Applied Sciences
ISSN:2289-5981 e-ISSN:2289-599X
UTM UNIVERSITI TEKNOLOGI MALAYSIA

Effect of dopants [Gd^{3+}, Sm^{3+}, Ca^{2+}, Sr^{2+} and Ba^{2+}] on the performance characteristics of ceria based electrolytes for application in solid oxide fuel cells

M.L. Reni and A. Samson Nesaraj*

Department of Chemistry, School of Science and Humanities, Karunya University, Karunya Nagar, Coimbatore - 641 114, Tamil Nadu, India
**Corresponding Author: drsamson@karunya.edu (A. Samson Nesaraj)*

Article history :
Received 21 March 2014
Revised 1 May 2014
Accepted 19 May 2014
Available online 1 June 2014

GRAPHICAL ABSTRACT

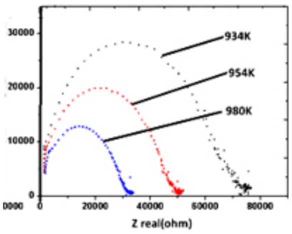

ABSTRACT

Doped CeO_2based materials are now-a-days proposed as alternate electrolyte materials for solid oxide fuel cells (SOFCs) working at low temperature (~723 – 873 K). In this research work, nanoparticles of CeO_2 doped with Gd^{3+}, Sm^{3+}, Ca^{2+}, Sr^{2+} and Ba^{2+}were prepared by a simple homogeneous chemical precipitation method. The prepared materials (after heat treatment at 1023 K for 2 hours) were systematically characterized by XRD, EDAX analysis, FTIR, particle size analysis and SEM. Lattice parameters were calculated from the XRD data. The XRD results indicatethat all the doped ceriasamples studied are single phase with a cubic fluorite structure. The average particle size of the doped ceria powder was about 48 – 115 nm and the particles haveshown narrow particle size distribution patterns. AC impedance spectroscopy studies performed on the sintered specimens have shown better oxide ion conductivity values and hence these materials may be suitable for application as electrolyte materials in solid oxide fuel cells working at low temperature (~723 – 873 K).

Keywords: Doped ceria based electrolytes, physical and electrical characterization, solid oxide fuel cells, low temperature application

http://dx.doi.org/10.11113/mjfas.v10n2.258

1. INTRODUCTION

Solid oxide fuel cell (SOFC) is an electrochemical device which converts chemical energy of a fuel to electrical energy at high efficiencies without harmful emissions [1-3].Conventional SOFCs use yttria-stabilized zirconia (YSZ) as an electrolyte. However, in order to obtain high enough current densities and to attain a useful power output, YSZ-based SOFCs must be operated at high temperature around 1273K. This high temperature of operation shows some disadvantages for commercialization, i.e., long-term stability of the cell and component materials, fabrication cost, etc. Therefore, many efforts have been made recently to reduce the operating temperature of SOFC. One effective method is to replace YSZ with doped ceria electrolytes that exhibit superior ionic conductivity at intermediate temperature range (773–1073K) [4-6]. CeO_2-based ceramics doped with suitable cations are considered as good oxygen ion conductors [7-9]. It has been reported that Sm^{3+} and Gd^{3+} have significant importance in conductivity of cerium oxide, when it is doped. The percentage composition and nature of the dopant affects the conductivity of cerium oxide [4]. Our group has made considerable effort in the development of doped ceria materials for application in SOFCs earlier [10-12]. In this research work, a set of doped ceria materials, namely, $Ce_{0.9}Gd_{0.1}O_{2-\delta}$,$Ce_{0.9}Sm_{0.1}O_{2-\delta}$,$Ce_{0.9}Ca_{0.1}O_{2-\delta}$,$Ce_{0.9}Sr_{0.1}O_{2-\delta}$ and $Ce_{0.9}Ba_{0.1}O_{2-\delta}$ weresynthesizedby the co-precipitation technique and their properties such as, crystalline characteristics, particulate behaviour and electrical characteristics were analyzed in order to make them suitable electrolytes for low temperature SOFCs (LTSOFCs). Study of dopants (especially 10 mole %) such as Gd^{3+}, Sm^{3+}, Ca^{2+}, Sr^{2+} and Ba^{2+} on the physico-chemical characteristics of ceria ceramics is very limited. Hence, our research group has attempted to study the physico-chemical properties of doped ceria ceramics for application in SOFCs in this research work and the findings are reported and discussed.

2. EXPERIMENTAL

2.1 Materials used

The chemicals used in the preparative method are: $Ce(NO_3)_3.6H_2O$(99.0%, Himedia, India), Gd_2O_3 (99.9%, LobaChemie, India), Sm_2O_3 (99.9%, LobaChemie, India), $Ca(NO_3)_2.4H_2O$, (Merck, India, 99%), $Ba(NO_3)_2$, (Qualigens, India, 98%), $Sr(NO_3)_2$, (99%, Nice, India) and NaOH (≥97%, Merck, India).

2.2 Preparation of $Ce_{0.9}Gd_{0.1}O_{2-\delta}$,$Ce_{0.9}Sm_{0.1}O_{2-\delta}$, $Ce_{0.9}Ca_{0.1}O_{2-\delta}$, $Ce_{0.9}Sr_{0.1}O_{2-\delta}$ and $Ce_{0.9}Ba_{0.1}O_{2-\delta}$ nanoparticles by chemical precipitation

Doped cerium dioxide (CeO_2) powder with composition $Ce_{0.9}Gd_{0.1}O_{2-\delta}$, $Ce_{0.9}Sm_{0.1}O_{2-\delta}$, $Ce_{0.9}Ca_{0.1}O_{2-\delta}$, $Ce_{0.9}Sr_{0.1}O_{2-\delta}$ and $Ce_{0.9}Ba_{0.1}O_{2-\delta}$ were prepared by chemical precipitation route using cerium nitrate, gadolinium nitrate (Gd_2O_3 is converted in to $Gd(NO_3)_3$ with the addition of HNO_3), samarium nitrate (Sm_2O_3 is converted in to $Sm(NO_3)_3$ with the addition of HNO_3), calcium nitrate, strontium nitrate and barium nitrate as starting materials. Calculated amount of starting materials were taken and dissolved in water. To which appropriate quantity of sodium hydroxide solution was added drop-wise and the solution was stirred continuously to complete precipitation under controlled alkaline pH range. The pH of the solution was adjusted in range of 11 – 14 by the addition of sodium hydroxide pellet. Afterwards, the mixture was stirred for about 2 h and the resultant yellow coloured precipitate [($Ce(OH)_4$ + $Gd(OH)_3$) or ($Ce(OH)_4$ + $Y(OH)_3$) or ($Ce(OH)_4$ + $Sr(OH)_2$)or ($Ce(OH)_4$ + $Ca(OH)_2$) or ($Ce(OH)_4$ + $Ba(OH)_2$)] was filtered. The resulting precipitate was filtered, washed with water and ethanol mixture (volume ratio 9:1) three times and dried at 328 K. Then, the powder was calcined at 573, 723, 873 and 1023 K for 2 hours each to get phase pure doped ceria nanoparticles. Figure 1.0 shows the schematic illustration of the synthesis of $Ce_{0.9}Gd_{0.1}O_{2-\delta}$, $Ce_{0.9}Sm_{0.1}O_{2-\delta}$, $Ce_{0.9}Ca_{0.1}O_{2-\delta}$, $Ce_{0.9}Sr_{0.1}O_{2-\delta}$ and $Ce_{0.9}Ba_{0.1}O_{2-\delta}$ by the chemical precipitation process. Main reactions occur during the experimental procedure can be written briefly as follows:

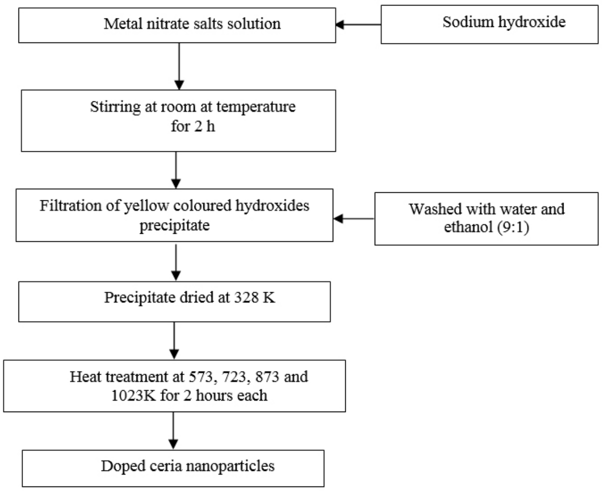

Fig. 1 Schematic representation of the synthesis of doped ceria nano particles by a chemical precipitation method.

Reaction mechanism for $Ce_{0.9}Gd_{0.1}O_{2-\delta}$ /$Ce_{0.9}Sm_{0.1}O_{2-\delta}$:

$$0.9\ Ce^{3+}_{(aq)} + 0.1\ Gd^{3+}/Sm^{3+}_{(aq)} + 3.9OH^{-}_{(aq)} + xH_2O_{\ (aq} \rightarrow 0.9Ce(OH)_4 .x\ H_2O_{(s)}\downarrow + 0.1\ Gd/Sm(OH)_3.x\ H_2O_{(s)}\downarrow,$$

323- 373 K

$$0.9\ Ce(OH)_4.xH_2O_{(s)} + 0.1\ Gd/Sm(OH)_3.x\ H_2O_{(s)} \rightarrow 0.9\ Ce(OH)_{4(s)} + 0.1\ Gd/Sm(OH)_{3(s)} + x\ H_2O_{(g)}\uparrow,$$

573 K / 723 K / 873 K / 1023 K for 2 hours

$$0.9\ Ce(OH)_{4(s)} + 0.1\ Gd/Sm(OH)_{3(s)} \rightarrow Ce_{0.9}Gd_{0.1}O_{2-\delta} /Ce_{0.9}Sm_{0.1}O_{2-\delta} + x\ H_2O_{(g)}\uparrow$$

Reaction mechanism for $Ce_{0.9}Sr_{0.1}O_{2-\delta}$/$Ce_{0.9}Ca_{0.1}O_{2-\delta}$/$Ce_{0.9}Ba_{0.1}O_{2-\delta}$:

$$0.9\ Ce^{3+}_{(aq)} + 0.1Sr^{2+}/Ca^{2+}/Ba^{2+}_{(aq)} + 3.8\ OH^{-}_{(aq)} + xH_2O_{\ (aq)} \rightarrow 0.9Ce(OH)_4 .x\ H_2O_{(s)}\downarrow + 0.1\ Sr/Ca/Ba(OH)_2.x\ H_2O_{(s)}\downarrow,$$

323 – 373 K

$$0.9\ Ce(OH)_4.xH_2O_{(s)} + 0.1\ Sr/Ca/Ba(OH)_2.x\ H_2O_{(s)} \rightarrow 0.9\ Ce(OH)_{4(s)} + 0.1\ Sr/Ca/Ba(OH)_{2(s)} + x\ H_2O_{(g)}\uparrow,$$

573 K / 723 K / 873 K / 1023 K for 2 hours

$$0.9\ Ce(OH)_{4(s)} + 0.1\ Sr/Ca/Ba(OH)_{2(s)} \rightarrow Ce_{0.9}Sr_{0.1}O_{2-\delta} /Ce_{0.9}Ca_{0.1}O_{2-\delta} /Ce_{0.9}Ba_{0.1}O_{2-\delta} + x\ H_2O_{(g)}\uparrow$$

2.3 Instruments handled

The powder XRD studies were carried out using a Shimadzu XRD6000 X-ray diffractometer at a scan speed of 5 degrees minute^{-1} using CuKα radiation. The lattice parameters were calculated by least square fitting method using DOS computer programming. The theoretical density of the powders was calculated with the obtained XRD data. The crystallite sizes of the powder were calculated by Scherrer's formula. EDAX analysis was performed with JEOL Model JSM-6360 to find out the percentage of elements present in the samples. Bruker IFS 66V FT-IR spectrometer was employed to record the FTIR spectra of doped CeO_2 powder in the range of 4000 – 400 cm^{-1}. The particle size of the powder was measured using Malvern Particle Size Analyzer using triple distilled water as medium. The surface morphology of the particles was studied by means of JEOL Model JSM-6360 scanning electron microscope.

The prepared powders were pressed (at 3000 psi) into disk type specimens (8 mm diameter x 1.5 mm thickness) with addition of binder. Then, the pressed specimens were sintered at 750 ºC for 5 h in air. The A.C. conductivity of these pellets was obtained using two probe A.C. impedance spectroscopy. Before measurements, the specimen was pressed in between two golden foils and connected with the conductivity set up. Measurements were made from ~800 – 950 K in air using a frequency response analyser Schlumberger, SI 1255) attached with an electrochemical interface, 1286 (Solatron Schlumberger). The amplitude of AC signal imposed on the specimens was about 500 mV. Current collectors were gold mesh and current leads were platinum wires.

3. RESULTS & DISCUSSION

3.1 XRD data

The XRD patterns of the Gd / Sm / Sr / Ca / Ba doped CeO$_2$ powder prepared by the chemical precipitation method with are shown in Figure 2. The XRD diffraction patterns of the synthesized samples have close resemblance with the standard JCPDS data (JCPDS No. 34-394) and there was no peak corresponding to any impurity in the samples. The crystalline properties obtained on doped ceria materials are reported in Table 1. The XRD patterns indicate that all the doped ceria samples studied are single phase with a cubic fluorite structure like pure CeO$_2$ as reported in the literature [13-14]. The unit cell parameter of doped ceria materials is higher than that of pure CeO$_2$ for all substituent's, which is in good agreement with the reported data [15]. The unit cell volumes calculated for the doped ceria particles are almost similar. The theoretical density of doped ceria materials is found to be in the range of 6.70 to 7.21 g/cc. The theoretical density of Sm – doped ceria was reported as 7.12 g/cc [16] which is comparable to our reported data.

3.2 EDAX data

The EDAX spectra obtained on doped ceria powder particlesare reported in Figure 3. The chemical composition data derived for the samples from EDAX analysis is indicated in Table 2. This experiment was performed to know about the percentage of atomic elements present in all the samples. Ce/Ba/O had shown variation in molar ratio due to the solubility differences of hydroxides as reported [17].

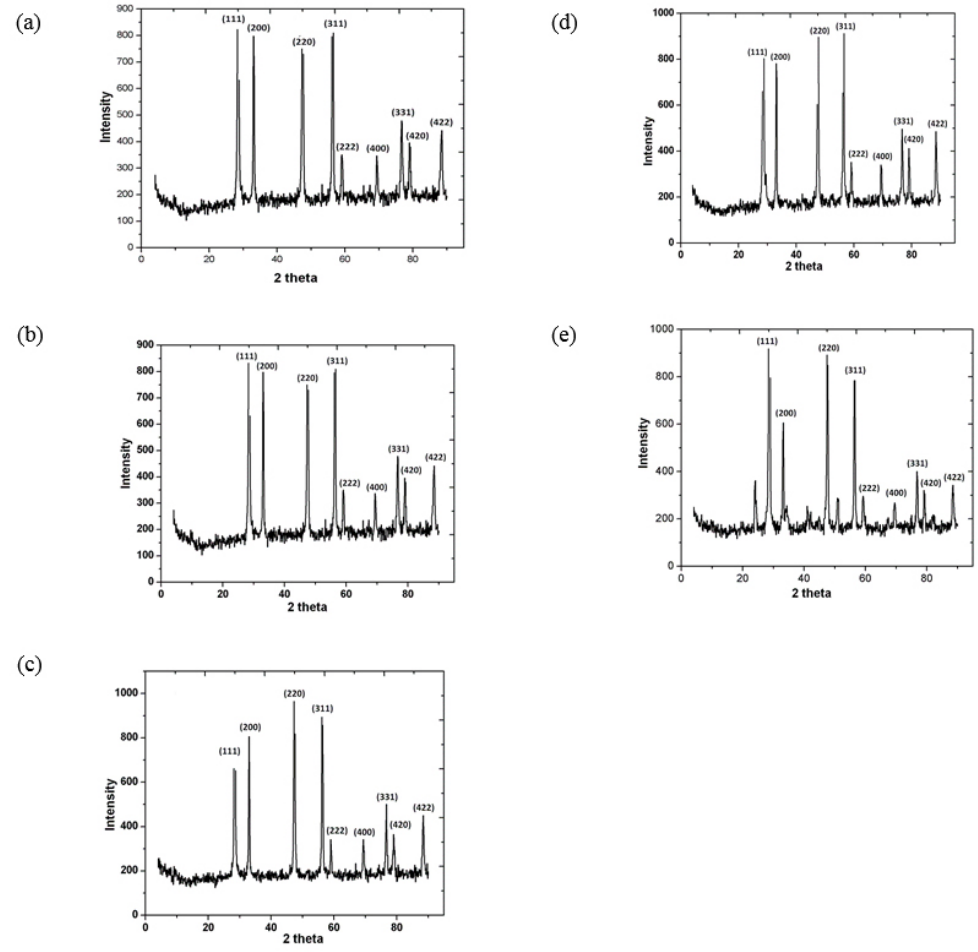

Fig. 2 XRD patterns obtained on calcined doped CeO$_2$ nanoparticles prepared by chemical precipitation method (a) $Ce_{0.9}Gd_{0.1}O_{2-\delta}$, (b) $Ce_{0.9}Sm_{0.1}O_{2-\delta}$, (c) $Ce_{0.9}Ca_{0.1}O_{2-\delta}$, (d) $Ce_{0.9}Sr_{0.1}O_{2-\delta}$, and (e) $Ce_{0.9}Ba_{0.1}O_{2-\delta}$

Table 1 Crystallographic parameters obtained on doped ceria nanoparticles

Sample	**Standard XRD data for CeO_2 powder (JCPDS No.34-394)**	**$Ce_{0.9}Gd_{0.1}O_{2-\delta}$**	**$Ce_{0.9}Sm_{0.1}O_{2-\delta}$**	**$Ce_{0.9}Ca_{0.1}O_{2-\delta}$**	**$Ce_{0.9}Sr_{0.1}O_{2-\delta}$**	**$Ce_{0.9}Ba_{0.1}O_{2-\delta}$**
Crystal structure	Cubic	Cubic	Cubic	Cubic	Cubic	Cubic
Unit cell lattice parameters (Å)	5.41134	5.42122	5.41837	5.41651	5.41660	5.41164
Unit cell volume (Å^3)	158.45	159.32	159.07	158.91	158.92	158.48
Theoretical density (g/cc)	7.2140	7.2127	7.1953	6.7080	6.9064	7.1337
Crystallite size (nm)	--	23.67	23.56	23.34	22.21	18.44

Table 2 EDAX data obtained on doped ceria powders

Sample	**Atomic percentage of elements**	**Molar ratio of elements after reaction**
$Ce_{0.9}Gd_{0.1}O_{2-\delta}$	Ce = 73.33 Gd = 8.20 O = 18.46	Ce = 0.9 Gd = 0.09 O = 1.989
$Ce_{0.9}Sm_{0.1}O_{2-\delta}$	Ce = 74.96 Sm = 5.72 O = 19.32	Ce = 0.9 Sm = 0.06 O = 2.03
$Ce_{0.9}Ca_{0.1}O_{2-\delta}$	Ce = 71.31 Ca = 2.79 O = 25.90	Ce = 0.9 Ca = 0.12 O = 2.86
$Ce_{0.9}Sr_{0.1}O_{2-\delta}$	Ce = 79.06 Sr = 3.32 O = 17.62	Ce = 0.9 Sr = 0.06 O = 1.757
$Ce_{0.9}Ba_{0.1}O_{2-\delta}$	Ce = 56.96 Ba = 22.99 O = 20.06	Ce = 0.9 Ba = 0.3 O = 2.73

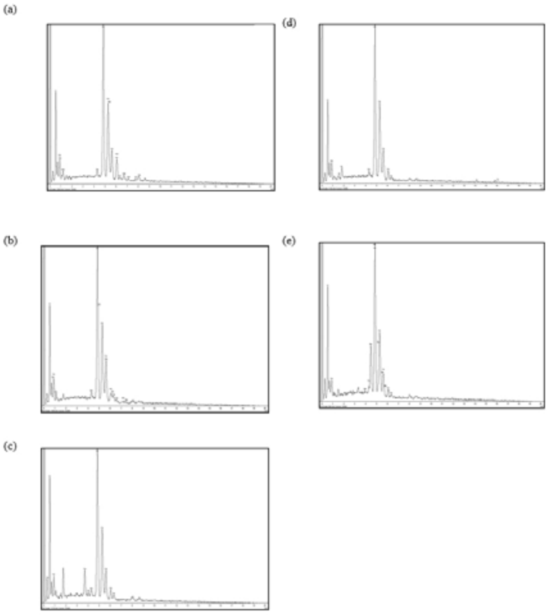

Fig. 3 EDAX obtained on calcined doped CeO_2 nanoparticles prepared by chemical precipitation method (a) $Ce_{0.9}Gd_{0.1}O_{2-\delta}$,(b) $Ce_{0.9}Sm_{0.1}O_{2-\delta}$, (c) $Ce_{0.9}Ca_{0.1}O_{2-\delta}$, (d) $Ce_{0.9}Sr_{0.1}O_{2-\delta}$, and (e) $Ce_{0.9}Ba_{0.1}O_{2-\delta}$

3.3 FTIR data

Figure 4.0 shows the FTIR spectra obtained on doped CeO_2 nanoparticles prepared by chemical precipitation method. FTIR measurements were done using the KBr method at RT. According to the standard IR spectra, peaks appeared at around 1400 and 500 cm^{-1} as well as the shoulder peaks that appear around 1500 – 1700 cm^{-1} are attributed to Ce-O vibration mode [18]. The broad peaks which are appeared at around 3400 cm^{-1} are related to the O-H stretching vibration of H_2O in the samples [19]. Figure 4(a) shown peak at 400 and 540 cm^{-1} which is due to Gd-O bond [20]. Figure 4(b), Figure 4(c), Figure 4(d) and Figure 4(e) had shown the peaks at 1250-1640cm^{-1}(Sm-O), 1420 - 1482 cm^{-1}(Ca-O), 600–700 cm^{-1}(Sr-O) and ≈474cm^{-1}(Ba-O) respectively[21-24].

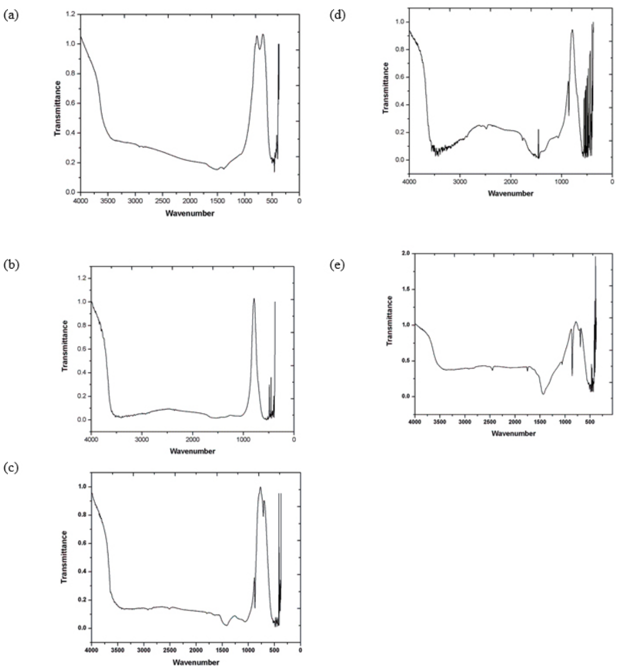

Fig. 4 FTIR spectra obtained on calcined doped CeO_2 nanoparticles prepared by chemical precipitation method (a) $Ce_{0.9}Gd_{0.1}O_{2-\delta}$(b) $Ce_{0.9}Sm_{0.1}O_{2-\delta}$, (c) $Ce_{0.9}Ca_{0.1}O_{2-\delta}$, (d) $Ce_{0.9}Sr_{0.1}O_{2-\delta}$, and (e) $Ce_{0.9}Ba_{0.1}O_{2-\delta}$

3.4 Particle characteristics

The prepared doped ceria particles were subjected to particle size measurements using Malvern particle size analyzer with triple distilled water as medium. For all the measurement, the samples were sonicated in triple distilled water before subjecting them for particle size measurements. The particle size distribution curves obtained on doped ceria samples prepared by chemical precipitation method are shown in Figure 5.0. The particle characteristics are indicated in Table 3.0. From the particle characteristics data, it was understood that the average particle size of doped ceria powder prepared by chemical precipitation method is found between nm and µm. The larger particles present in the samples may be due to the agglomeration effect during high temperature treatment.

Table 3 Particle characteristics data obtained on doped ceria nanoparticles prepared by chemical precipitation method

Sample	Peak 1		Peak 2		APS** (nm)
	% intensity	D* (nm)	% intensity	D (nm)	
$Ce_{0.9}Gd_{0.1}O_{2-\delta}$	95.6	7.924	4.4	2325	6.654
$Ce_{0.9}Sm_{0.1}O_{2-\delta}$	98.3	4.003	1.7	2710	3.189
$Ce_{0.9}Ca_{0.1}O_{2-\delta}$	100.0	887.6	--	--	3212
$Ce_{0.9}Sr_{0.1}O_{2-\delta}$	100.0	904.2	--	--	1093
$Ce_{0.9}Ba_{0.1}O_{2-\delta}$	100.0	783.5	--	--	2032

** D: Diameter; **APS: Average Particle Size*

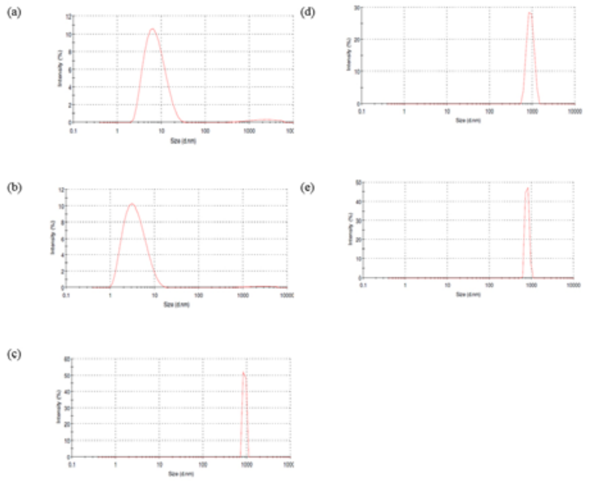

Fig. 5 Particle distribution curves obtained on calcined doped CeO_2 nanoparticles prepared by chemical precipitation method (a) $Ce_{0.9}Gd_{0.1}O_{2-\delta}$, (b) $Ce_{0.9}Sm_{0.1}O_{2-\delta}$, (c) $Ce_{0.9}Ca_{0.1}O_{2-\delta}$, (d) $Ce_{0.9}Sr_{0.1}O_{2-\delta}$, and (e) $Ce_{0.9}Ba_{0.1}O_{2-\delta}$

3.5 SEM data

The scanning electron microscopic (SEM) photographs obtained on calcineddoped ceria nanoparticles prepared by chemical precipitation method are shown in Figure 6.0**.** From the micrographs, it was understood that the particles are present in the range of 48 – 115 nm. The average grain size is found to be in the range of 75 nm. The presence of large sized particles in the samples may be due to the agglomeration during high temperature treatment. Also, the micrographs reveal the fluffy nature of the samples. All the samples found to be porous. In all the samples, well defined fine grains are uniformly distributed. The difference in particle size analyzer and SEM is that, particle size analyzer detect hydrodynamic diameter of the aggregated particles.

3.6 Electrical conductivity measurements

Figure 7.0 shows the impedance spectra of doped ceria electrolyte specimens at different temperatures. The frequency range for all the spectra was found to be less than 200 kHz. From the plots, it is noted that as the temperature is increased, the time constants of the relaxations resulting from the individual polarizations are reduced and the arcs are shifted to higher frequencies as reported in literature [25]. Reports on ionic conductivity measurements for ceria solid solutions are difficult to interpret because many authors have not separated the bulk and grain boundary contributions to the total conductivity. This is particularly troublesome for ceria solid solutions as the segregation of dopants/impurities to external and internal (grain boundary) can occur [26]. From the impedance plots, the individual resistance R_i can be converted to conductivity, $\sigma_i$using the equation $\sigma_i = l/SR_i$, where 'l' is the sample thickness and 'S' the electrode area of the sample surface. The conductivity values were calculated and reported in Table 4.0.

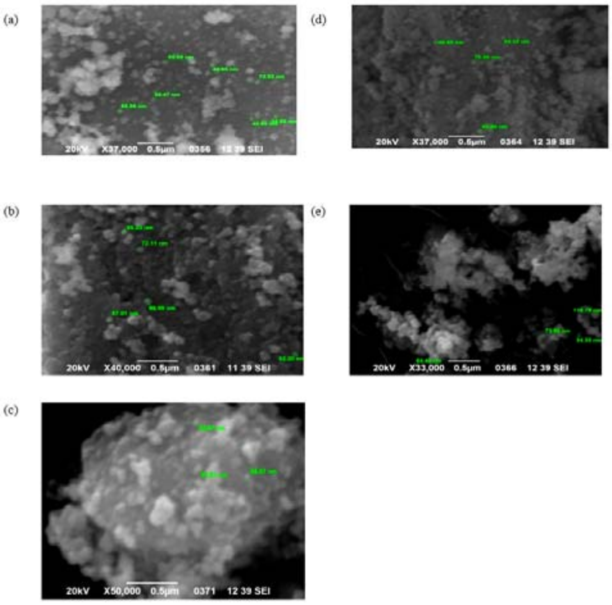

Fig. 6 SEM photographs obtained on calcined doped CeO_2 nanoparticles prepared by chemical precipitation method (a) $Ce_{0.9}Gd_{0.1}O_{2-\delta}$(b) $Ce_{0.9}Sm_{0.1}O_{2-\delta}$, (c) $Ce_{0.9}Ca_{0.1}O_{2-\delta}$, (d) $Ce_{0.9}Sr_{0.1}O_{2-\delta}$, and (e) $Ce_{0.9}Ba_{0.1}O_{2-\delta}$

The temperature dependence of electrical conductivity is expressed by the Arrhenius equation, $\sigma = A/T \exp(-E_a/KT)$. From the oxide ion conductivity data, it is noted that the oxide-ion conductivity values were increased with increasing temperature. The Arrhenius plots drawn for all the specimens (log σ Vs 1000/T) are indicated in Figure 8.0. The slope of the log σ Vs. 1000/T gives the activation energy (fig.8.0), E_a. The activation energy of all the doped ceria specimens is calculated and indicated in Table 4.0. The activation energies of all the specimens are higher than (0.78 eV) reported in literature [27-28].

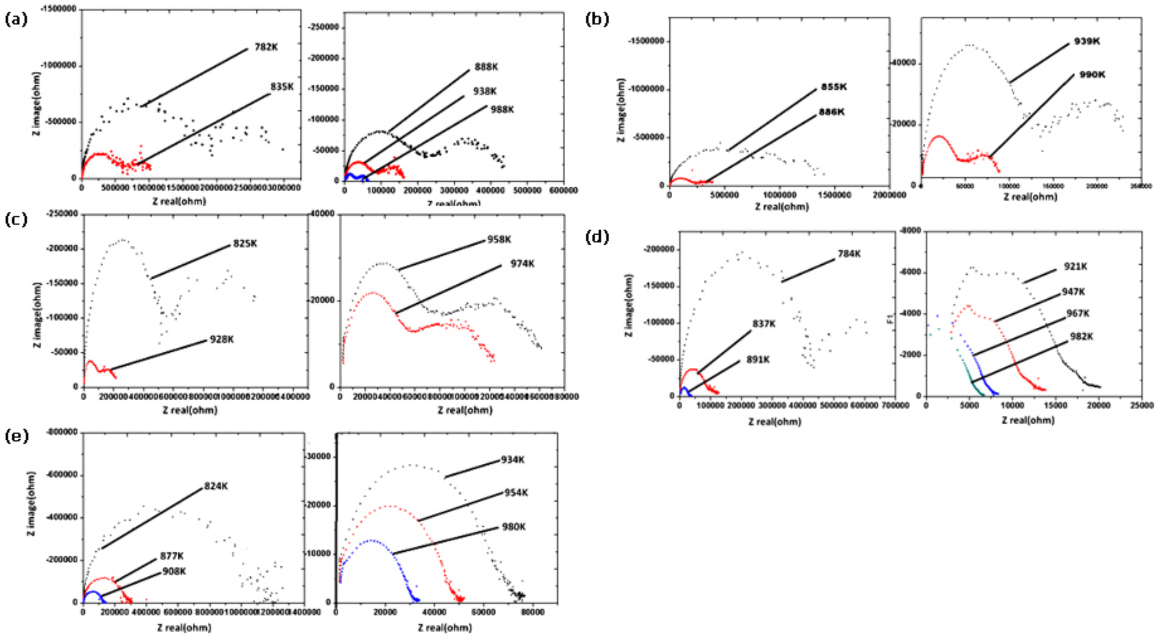

Fig. 7 AC impedance spectra obtained on sintered doped CeO_2 specimens at different temperatures (a) $Ce_{0.9}Gd_{0.1}O_{2-\delta}$, (b) $Ce_{0.9}Sm_{0.1}O_{2-\delta}$, (c) $Ce_{0.9}Ca_{0.1}O_{2-\delta}$, (d) $Ce_{0.9}Sr_{0.1}O_{2-\delta}$, and (e) $Ce_{0.9}Ba_{0.1}O_{2-\delta}$

Table 4 Electrical properties obtained on sintered doped ceria specimens

Sample	**Temperature in K**	**Oxide ion Conductivity (Sm^{-1})**	**Log (conductivity)**	**1000/T**	**Activation Energy (eV)**
$Ce_{0.9}Gd_{0.1}O_{2-\delta}$	782	$9.1889x10^{-6}$	-5.0367	1.27877	0.028662
	835	$3.7859x10^{-5}$	-4.4218	1.19760	
	888	$8.0545x10^{-5}$	-4.09396	1.126126	
	938	$2.024777x10^{-4}$	-3.6936	1.066098	
	988	$4.8997x10^{-4}$	-3.3098	1.012146	
$Ce_{0.9}Sm_{0.1}O_{2-\delta}$	855	$9.85946x10^{-5}$	-4.0061	1.16959	0.033118
	886	$1.8185x10^{-4}$	-3.7402	1.128668	
	939	$3.4486x10^{-4}$	-3.46235	1.06496	
	990	$9.44435x10^{-4}$	-3.02487	1.0101	
$Ce_{0.9}Ca_{0.1}O_{2-\delta}$	825	$6.71414x10^{-5}$	-4.1730	1.21212	0.087911
	928	$3.7864x10^{-4}$	-3.42178	1.07759	
	958	$4.4877x10^{-4}$	-3.34798	1.04384	
	974	$4.49924x10^{-4}$	-3.34686	1.026694	
$Ce_{0.9}Sr_{0.1}O_{2-\delta}$	784	$7.52231x10^{-5}$	-4.12365	1.2755	0.0306967
	837	$3.49832x10^{-4}$	-3.45614	1.19474	
	891	$1.064596x10^{-3}$	-2.97281	1.12233	
	921	$1.8238x10^{-3}$	-2.7390	1.085776	
	947	$2.99863x10^{-3}$	-2.5231	1.055966	
	967	$3.46287x10^{-3}$	-2.46056	1.03413	
	982	$5.15233x10^{-3}$	-2.28799	1.018329	
$Ce_{0.9}Ba_{0.1}O_{2-\delta}$	824	$3.25640x10^{-5}$	-4.48726	1.21359	0.0236490
	877	$1.289984x10^{-4}$	-3.88942	1.14025	
	908	$2.8581994x10^{-4}$	-3.5439	1.101322	
	934	$5.22503x10^{-4}$	-3.2819	1.070664	

The electrical conductivity values of doped electrolyte specimens were less than the reported data [29-30]. It is reported that the ceria based ceramic comes out as a highly dense specimen (over 98% theoretical density) when sintered at 1773 K [31]. In this research work, the doped ceria specimens were sintered only at 923 K for 5 h. By increasing the sintering temperature, the oxide ion conductivity of doped ceria specimens can be improved to some extent. Among the five samples studied, $Ce_{0.9}Sr_{0.1}O_{2-\delta}$ shows 5.15233 x 10^{-3} S/m at 982 K when compared with all other specimens. From the conductivity data, it was understood that the specimens should be sintered at high temperature (>1000k for long duration) to get more conductivity values as reported in the literature [31]. However, the conductivity values were not changed much with variation in dopant concentration. Further, it was reported that high activation energy may restrict the final ionic conductivity [32].

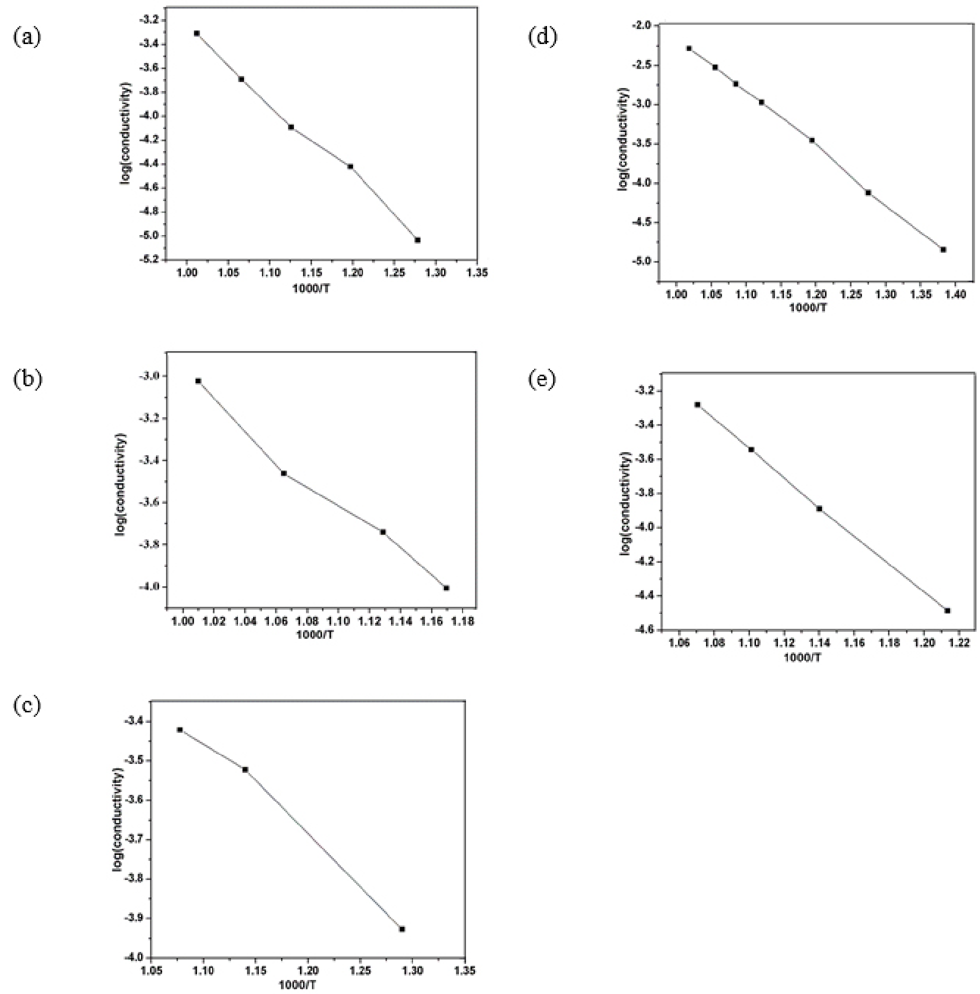

Fig. 8 Arrhenius plots obtained on sintered doped CeO$_2$ specimens (a) Ce$_{0.9}$Gd$_{0.1}$O$_{2-\delta}$, (b) Ce$_{0.9}$Sm$_{0.1}$O$_{2-\delta}$, (c) Ce$_{0.9}$Ca$_{0.1}$O$_{2-\delta}$, (d) Ce$_{0.9}$Sr$_{0.1}$O$_{2-\delta}$, and (e) Ce$_{0.9}$Ba$_{0.1}$O$_{2-\delta}$

3. CONCLUSION

CeO$_2$ nanoparticles doped with Gd, Sm, Ca, Sr and Ba have been synthesized by homogeneous chemical precipitation method and their performance characteristics are reported. The XRD patterns of all the doped CeO$_2$ particles indicate the fluorite cubic crystal structure. The EDAX data confirmed the presence of required elements in all the samples. The characteristics peaks of CeO$_2$ are confirmed by FTIR spectroscopy in all the samples. The particulate properties confirmed the presence of nanoparticles in the samples. Sr doped CeO$_2$ has shown better electrical characteristics when compared with other sintered specimens. Hence, it may be used as an alternate electrolyte material in LTSOFCs.

ACKNOWLEDGEMENT

The authors thank the management of Karunya University for promoting high temperature fuel cell research activity in the Department of Chemistry. Also, the authors wish to thank the HOD, Department of Chemistry, Karunya University for his encouragement to publish this research work.

REFERENCES

[1] A.Stamatis, C.Vinni, D.Bakalis, F.Tzorbatzoglou, P. Tsiakaras, Energies. 5 (2012) 4268.

[2] M.S.Y. Ebaid, M.Y. Mustafa, Jordan J. Mech. Indus. Eng. 5 (2011) 185.

[3] M. Cimenti, J.M. Hill, Energies. 2 (2009) 377.

[4] S. Zha, C. Xia, G.Meng, J. Power Sources. 115 (2003) 44.

[5] M. Nakayama, M. Martin, Phy. Chem. Chem. Phys. 11 (2009) 3241.
[6] Y.-P. Fu, S.-H. Chen, Ceram.Int. 36 (2010) 483.
[7] Z.Tianshu, P.Hing, H.Huang, J. Kilner, Solid State Ionics. 148 (2002) 567.
[8] T. Kudo, H. Obayashi, J. Electrochem. Soc. 123 (1976) 415.
[9] F.-Y.Wang, B.-Z.Wan, S.Cheng, J. Solid State Electrochem. 9 (2005) 168.
[10] A.S.Nesaraj, I. Arul Raj, R. Pattabiraman, J. Iran. Chem. Soc. 7 (2010) 564.
[11] J.J. Ketzial, A.S. Nesaraj, J. Ceram. Process. Res. 12 (2011) 74.
[12] D.Radhika, A.S.Nesaraj, Asian J. Res. Chem. 4 (2011) 1447.
[13] X. Guan, H. Zhou, Z. Liu, Y. Wang, J. Zhang, Mater. Res. Bull. 43 (2008) 1046.
[14] Y.D. Zhena, A.I.Y. Tok, S.P. Jiang, F.Y.C. Boey, J. Power Sources. 178 (2008) 69.
[15] S. Dikmen, J. Alloy. Compd. 491 (2010) 106.
[16] V. Singh, S. Babu, A.S.Karakoti, A. Agarwal, S. Seal, J. Nanosci. Nanotechnol. 10 (2010) 1.
[17] T. Fanghänel, V. Nec, Pure Appl. Chem. 74 (2002) 1895.
[18] X. Chao, Z.Junwu, Y.Xujie, L.Hude, W. Xin, J. Rare Earth. 26 (2008) 51.
[19] J.Gao, F.Guan, Y.Ma, W.Yang, J.Kang, H.Deng, Y. Qi, Rare Metals. 20 (2001) 217.
[20] N. Dhananjaya, H.Nagabhushana, B. Mater. Sci. 35 (2012) 519.
[21] M.Y.Chenga, D.H.Hwanga, H.S. Sheub, B.J. Hwanga, J. Power Sources. 175 (2008) 137.
[22] S. Yan, M. Kim, S.O. Salley, K.Y.S. Ng, Appl. Catal. A-Gen. 360 (2009) 163.
[23] R. Wurm, O. Dernovsek, P. Greil, J. Mater. Sci. 34 (1999) 4031.
[24] Ardelean, M. Todera, J. Optoelectronic. Adv. Mater. 8 (2006)1118.
[25] Z. Zhan, T.L. Wen, H.Tu, Z.Y. Lu, J. Electrochem. Soc. 148 (2001) A 427 – A432.
[26] B.C.H. Steele, K. Zhang, R.A. Rudkin, N. Kiratzis, M. Christie, in: M. Dokiya, O. Yamamoto, H. Tagawa, S.C. Singhal (Eds.), Proc. Fourth International Symposium on Solid Oxide Fuel Cells, (SOFC-IV), NJ, 1995, p.1028.
[27] J.R. Jurado, J. Mater. Sci. 36 (2001) 1133.
[28] T. Ishihara, K. Sato, Y. Takita, J. Am. Ceram. Soc. 79 (1996) 913.
[29] M. Godickemeiner, K. Sasaki, L.J. Gauckler, in: M. Dokiya, O. Yamamoto, H. Tagawa, S.C. Singhal (Eds.), Proc. Fourth International Symposium on Solid Oxide Fuel Cells, (SOFC-IV), NJ, 1995, p.1072.
[30] M. Sahibsada, R.A. Rudkin, B.C.H. Steele, I.S. Metcalfe, J. A. Kilner, in: U. Stimming, S.C. Singhal, H. Tagawa, W. Lehner (Eds.), Proc. Fifth International Symposium on Solid Oxide Fuel Cells (SOFC-V), NJ, 1997, p. 244.
[31] Y.Gu, G.Li, G. Meng, D. Peng, Mater. Res. Bull. 35 (2000) 297.
[32] L. Fan, C. Wang, M. Chen, B. Zhu, J. Power Sources. 224 (2013) 154.